Intrinsic periodic and aperiodic stochastic resonance in an electrochemical cell

Ishant Tiwari, Richa Phogat, and P. Parmananda
Department of Physics, Indian Institute of Technology, Bombay, Powai, Mumbai-400 076, India

J. L. Ocampo-Espindola and M. Rivera
Centro de Investigación en Ciencias-(IICBA), UAEM, Avenida Universidad 1001, 62209 Cuernavaca, Morelos, México
(Received 28 March 2016; revised manuscript received 5 July 2016; published 12 August 2016)

In this paper we show the interaction of a composite of a periodic or aperiodic signal and intrinsic electrochemical noise with the nonlinear dynamics of an electrochemical cell configured to study the corrosion of iron in an acidic media. The anodic voltage setpoint (V_0) in the cell is chosen such that the anodic current (I) exhibits excitable fixed point behavior in the absence of noise. The subthreshold periodic (aperiodic) signal consists of a train of rectangular pulses with a fixed amplitude and width, separated by regular (irregular) time intervals. The irregular time intervals chosen are of deterministic and stochastic origins. The amplitude of the intrinsic internal noise, regulated by the concentration of chloride ions, is then monotonically increased, and the provoked dynamics are analyzed. The signal to noise ratio and the cross-correlation coefficient versus the chloride ions' concentration curves have a unimodal shape indicating the emergence of an intrinsic periodic or aperiodic stochastic resonance. The abscissa for the maxima of these unimodal curves correspond to the optimum value of intrinsic noise where maximum regularity of the invoked dynamics is observed. In the particular case of the intrinsic periodic stochastic resonance, the scanning electron microscope images for the electrode metal surfaces are shown for certain values of chloride ions' concentrations. These images, qualitatively, corroborate the emergence of order as a result of the interaction between the nonlinear dynamics and the composite signal.

DOI: 10.1103/PhysRevE.94.022210

Stochastic resonance (SR) is a phenomenon [1–3] wherein the presence of external noise enhances the detection of weak subthreshold signals in nonlinear dynamical systems. This combination of an external random signal and the forcing term has been studied exhaustively both theoretically and experimentally in diverse physical, chemical, and biological systems [4–9]. A comprehensive review by Gammaitoni*et al.* [10] highlights all the important advances in this field along with the prominent references. Another aspect of the constructive role of noise involves the inception of coherence in deterministic systems subjected to solely stochastic fluctuations. In this case the coherence resonance (CR) involves the inception of regular dynamics under the influence of purely stochastic external perturbations. In CR, similar to SR, there exists an optimum external noise amplitude where maximal regularity of the invoked dynamics is provoked. This effect of CR is also rather generic and consequently has been observed in a number of diverse systems [11–14]. Both SR and CR curves have the signature unimodal shape implying the existence of an optimum noise level where maximum regularity of the invoked dynamics is observed.

Considering the fact that in real dynamical systems noise is ubiquitous, the plausible constructive effects may be of interest to the research community. There have been previous studies of the interaction of internal noise with various nonlinear systems [15], especially in biological systems where internal noise is an inseparable element of the system itself [16–20]. This paper is an extension to these previous studies while using an electrochemical cell. Earlier, we had reported the observation of intrinsic coherence resonance (ICR) in an electrochemical cell [21]. In this paper, amplitude of the intrinsic (internal) noise, regulated by the concentration of chloride ions, was monotonically increased, and the provoked dynamics analyzed. The experimentally constructed coherence factor β versus concentration of the chloride ions' curve had a unimodal shape indicating the emergence of ICR. These experimental results were subsequently corroborated [22], exploring in detail the chemical conditions necessary to observe the ICR phenomenon.

In the present paper, we report the experimental observation of internal stochastic resonance in an electrochemical cell. Two different scenarios have been considered for the subthreshold signal, namely, periodic and aperiodic. The amount of internal noise was again regulated by the concentration of chloride ions in the electrolytic solution. These chloride ions attack the metal surface stochastically through a process, known in electrochemistry literature, as pitting corrosion [23,24]. The addition of chloride ions does not have any significant deterministic effect on the dynamics of the original system as can be seen in Fig. 1 from Ref. [21] in which the effect of chloride ions on the system was analyzed for the purposes of studying coherence resonance. In Fig. 1 panels (a) and (e) of Ref. [21], the system response is almost identical both for low as well as very high levels of the chloride ions' concentration. Had there been any significant deterministic contribution of the chloride ion to the system response (shifting of bifurcations and introduction of new steady states) it would have manifested itself in the time series presented in this Fig. 1 panels (a) and (e). The absence of any such features indicates that addition of chloride ions is tantamount to adding noise because the provoked pitting corrosion is largely accepted to be a stochastic process. Therefore, increasing the concentration of chloride ions increases this stochastic activity (increased levels of internal noise), resulting in enhanced levels of pitting corrosion. It was observed that an appropriate amount of internal noise can indeed facilitate the transfer of information and the provoked system dynamics exhibit ISR (periodic and aperiodic) as a function of the concentration of chloride ions

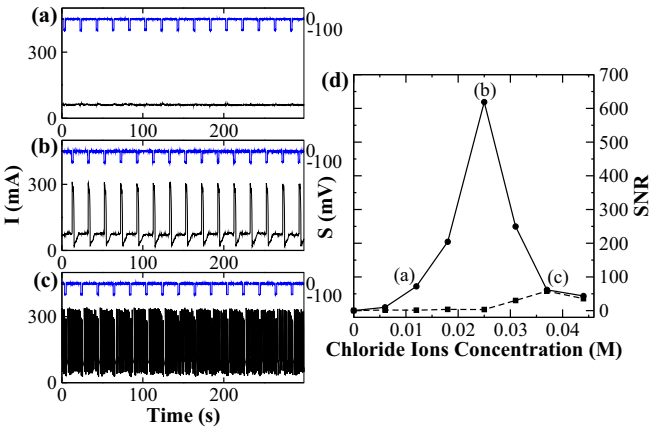

FIG. 1. Intrinsic noise-induced system response in the anodic current I for (a) low, (b) medium, and (c) high levels of internal noise superimposed to a subthreshold periodic signal. The setpoint for the autonomous system is $V_0 = 650$ mV, and the threshold value is $V_{hc} = 500$ mV. The perturbation amplitude is $A = -100$ mV, the time period between pulses is 20 s, and the pulse duration is 2 s. The corresponding chloride ions' concentrations are 0.0125, 0.0249, and 0.0373 M, respectively. (d) The experimentally generated SNR curves as a function of noise level (chloride ions' concentration) for the subthreshold periodic signal perturbation (continuous line) and in the absence of a subthreshold signal [$S(t) = 0$, dashed line]. The indicated points (a)–(c) located on the continuous line correspond to the anodic current time series shown in the left panels. These curves have unimodal shapes confirming the emergence of intrinsic periodic stochastic resonance (IPSR) and ICR, respectively.

present in the electrolytic solution. This inception of ISR is furthermore verified quantitatively by calculating the signal to noise ratio (SNR) and the cross-correlation coefficient (CCC) for the periodic and aperiodic scenarios, respectively. In an effort to compare the regularity observed in the time series with the roughness of the metal surface (periodic scenario) a scanning electron microscope (SEM) imaging of the anode is carried out to visualize the surface morphology of the anode surface undergoing pitting corrosion.

The experimental system consists of a three electrode electrochemical cell configured to study the potentiostatic electrodissolution of iron in an acidic solution [21,25]. The anode (working electrode) was a high purity iron disk embedded in epoxy, which was exposed to the solution at an initially finely polished cross-sectional surface, restricting the corrosion to take place only at the surface of the anode. The cathode (counterelectrode) was an inert conductive cylindrical rod partially immersed in the electrolytic solution, and the reference electrode was a saturated calomel electrode. All three electrodes were immersed in an electrolytic solution consisting of sulfuric acid and a sulfate salt. The anodic voltage (V) between the working and the reference electrode is adjusted continuously by a potentiostat (PINE Instrument Co.). For our experiments on intrinsic periodic or aperiodic stochastic resonance, this voltage consists of a setpoint voltage V_0 (setpoint) and the subthreshold periodic or aperiodic pulse train $S(t)$. This setpoint voltage is set by the potentiostat, and the pulse train is generated by a computer and applied using a USB control card attached to the external input of the potentiostat. The anodic current (I) was simultaneously recorded using a 16 bit USB data acquisition card with a sampling rate of 1 KHz. In order to provide an internal source of noise [21,22], a fixed amount of potassium chloride or sodium chloride, our source of chloride ions, was added to the electrolytic solution without changing the volume maintained in the electrochemical cell. Different (increasing) concentrations of chloride ions added to the electrolytic solution are considered, mimicking the monotonically increasing level of the internal noise. For every concentration of the chloride ions (experimental run) the surface of the anode is polished and cleansed in an effort to provide the same set of initial conditions to the anode.

For the periodic and aperiodic perturbation scenarios, two slightly different experimental specifications have been considered in order to analyze the anode's surface morphology and corroborate the robustness of our experimental observations with respect to changes in the working electrode size, its purity, the electrolytic solution, and the type of counterelectrode used. In the periodic scenario, the anode is a 6.3 mm diameter disk (99.98% Sigma-Aldrich), the cathode is a 5 mm graphite rod, and the electrolyte is a mixture of 1 M sulfuric acid and 0.4 M potassium sulfate. In comparison, for the aperiodic scenario, the anode is a 7.6 mm diameter disk (99.95% Alfa Aesar), the cathode is a 5 mm copper rod, and the electrolyte is a mixture of 1 M sulfuric acid and 0.25 M cupric sulfate. In both cases a volume of 300 ml is maintained in the electrochemical cell, and all the experiments were carried out at room temperature (∼298 K). A schematic of the experimental setup with the three electrodes immersed in the electrolytic solution has been shown previously [25].

The analysis of the autonomous dynamics for a single iron electrode immersed in a solution of cupric sulfate and sulfuric acid, including the underlying bifurcations, has already been reported elsewhere [25]. It reveals the existence of an interval in parameter space wherein period one oscillations of anodic current (I) are found. This parameter interval is sandwiched between parameter domains where the anodic current dynamics exhibit fixed point behavior. Within the oscillatory region, relaxation oscillations were exhibited in which the period increased with an increase in the voltage. This increase in period as a function of the bifurcation parameter (anodic voltage) is characteristic of an underlying homoclinic bifurcation. Our previous study of this system [25] demonstrated that period lengthening occurs until oscillations cease at the homoclinic bifurcation point V_{hc}. For potentials greater than V_{hc}, the system shows excitable fixed point behavior, which has been experimentally demonstrated previously [25]. Similar regions have also been identified when the electrolyte is a mixture of potassium sulfate and sulfuric acid [21]. The exact location of these bifurcation points depends on the actual concentrations of the chemicals and the physical dimensions of the anode.

For our experiments on intrinsic periodic and aperiodic stochastic resonances, the setpoint voltage V_0 was chosen such that $V_0 > V_{hc}$ and consequently an excitable steady state behavior was observed. The anodic voltage V was then defined as $V = V_0 + S(t)$, where V_0 and the subthreshold periodic or aperiodic pulse train $S(t)$ were set such that $V = V_0 + S(t) > V_{hc}$, i.e., the subthreshold signal never shifts the system into the oscillatory regime. Prior to every experiment, the homoclinic

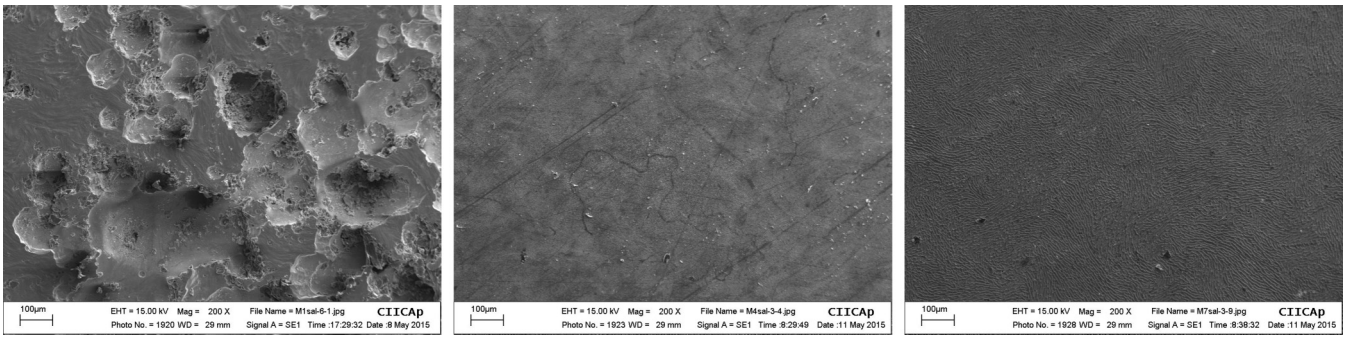

FIG. 2. SEM images, revealing the morphology of the anode surface at the conclusion of three experimental runs. The images from left to right correspond to the data-points (a)–(c) of the experimentally constructed SNR curve (continuous line) shown in Fig. 1(d). The corresponding time series are shown in the left panels of Fig. 1.

bifurcation point was identified to determine the maximum amplitude permitted for the perturbation $S(t)$.

For the first set of experiments, a subthreshold periodic pulse train was used. In this case the bifurcation point is located at $V_{\rm hc} = 500$ mV, so the pulse amplitude (constant) was chosen to be $A = -100$ mV and the setpoint was $V_0 = 650$ mV. The time between pulses was 20 s, and its duration was $\Delta t = 2$ s. Figures 1(a)– 1(c) show the time series of the system response (lower curves) with periodic subthreshold pulse trains (upper curves in blue) for three different levels of internal noise [increasing from (a)–(c)], determined by the chloride ions' concentration. We see in panel (a) that there is no response to the subthreshold signal at a low internal noise level, whereas there is excellent correspondence between the subthreshold signal and the system response at an optimum noise level as shown in panel (b). In panel (c), the subthreshold signal is completely lost in the system response due to the high levels of internal noise

In order to analyze the invoked dynamics, we use the SNR [26] to calculate the ratio of signal power to noise power. This measure is used to compare the amount of true signal versus the background noise and is defined by

$$\mathrm{SNR} = \frac{\sigma^2_{\rm signal}}{\sigma^2_{\rm noise}}. \qquad (1)$$

Panel (d) in Fig. 1 shows the experimentally generated SNR versus concentration of the chloride ions' (internal noise amplitude) curve. The computed curve (continuous line) has a unimodal shape indicating the observance of IPSR. It implies that for some optimum levels of internal noise the interplay of stochastic pitting process, provoked by the chloride ions, and the periodic subthreshold signal superimposed to the autonomous nonlinear dynamics invokes an optimal transfer of information as shown in panel (b). In contrast, at low levels of chloride concentrations, the noise provoked dynamics are devoid of any periodic features, exhibiting a noisy fixed point direct current response. Furthermore, at high levels of chloride concentrations, the dynamics are totally dominated by the stochastic component, losing completely the periodic profile of the subthreshold pulse train.

Additionally, Fig. 1(d) shows another experimentally generated SNR curve (dashed line) for an experimental run without the subthreshold periodic signal [$S(t) = 0$], maintaining the setpoint and bifucation parameters identically. This new curve also shows a unimodal shape indicating the emergence of ICR [21]. Comparing these curves we observe that: (a) the invoked order is considerably enhanced when the subthreshold periodic signal is present, and (b) the level of noise necessary for the emergence of order is larger in the absence of the periodic signal. The time series (not shown) corresponding to these experiments are consistent to the emergence of the ICR in the electrochemical system solely under the presence of internal noise.

Considering the periodic nature of the subthreshold perturbation we tried to correlate the enhanced transfer of information of the time series to the spatial organization of the anode morphology undergoing pitting corrosion. For these purposes, for some experimental runs, the anode disk was removed from the electrochemical cell and taken over to the SEM laboratory for imaging purposes. Figure 2 shows the images of the anode surface obtained using the SEM, corresponding to points (a)–(c) of the SNR curve shown in Fig. 1(d). The magnification factor (200×) is the same for all the samples. It is observed that the anode surface corresponding to data-point (b) of the SNR curve where maximum correlation in the noise-induced time series is observed exhibits increased homogeneity (smoothness) in the surface morphology. In contrast, the images corresponding to (a) low and (c) high levels of internal noise exhibit a substantially rougher morphology for the anode surface. This image analysis is a qualitative tool employed to support the results reported in Fig. 1.

For our second set of experiments a subthreshold aperiodic pulse train was considered using two different interspike intervals (ISIs). First, the time intervals between pulses were constructed by using a random number generator whose output, distributed in the interval $[-1,1]$, is consistent with white noise with a Gaussian distribution. Proper scaling and translating of the absolute values of these numbers were performed to generate the suitable ISI for our experiments. The pulse amplitude was chosen to be $A = -200$ mV, and the pulse duration was $\Delta t = 1$ s. Thus, whereas the amplitude and pulse duration remain constant, the interspike interval varies stochastically.

Figures 3(a)– 3(c) show the time series of the system response (lower curves) for identical stochastic subthreshold spike trains (upper curves in blue) for three different levels of chloride ions' concentrations (internal noise). We see in panel

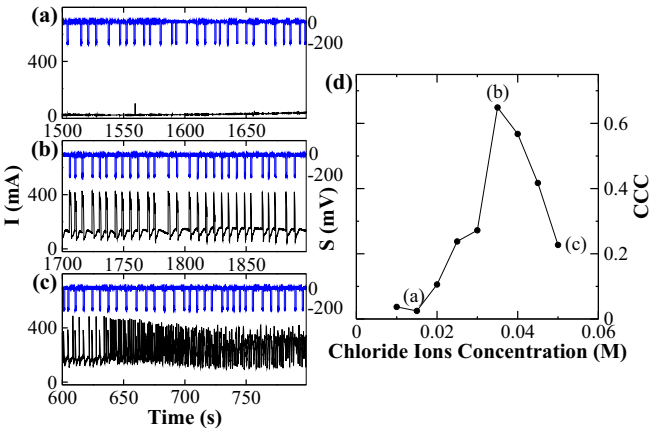

FIG. 3. Intrinsic noise-induced system response in the anodic current I for (a) low, (b) medium, and (c) high levels of internal noise superimposed to a subthreshold aperiodic signal with stochastic ISIs. The setpoint for the autonomous system is $V_0 = 610$ mV, and the threshold value is $V_{hc} = 320$ mV. The perturbation amplitude is $A = -200$ mV, and the pulse duration is 1 s. The corresponding chloride ions' concentrations are 0.015, 0.035, and 0.05 M, respectively. Notice that the representative portions of the time series, which are shown for each concentration, are of different times in the same subthreshold pulse. This is performed to show the best portion of the recorded time series. (d) The experimentally generated CCC as a function of noise level (chloride ions' concentration) for the subthreshold aperiodic signal perturbation. The indicated points (a)–(c) correspond to the anodic current time series shown in the left panels. This curve has a unimodal shape confirming the emergence of an intrinsic aperiodic stochastic resonance in the noise provoked dynamics.

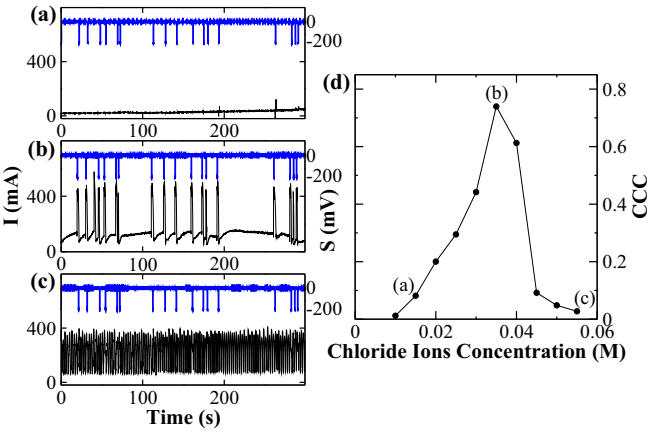

FIG. 4. Intrinsic noise-induced system response in the anodic current I for (a) low, (b) medium, and (c) high levels of internal noise superimposed to a subthreshold aperiodic signal with chaotic ISIs. The setpoint for the autonomous system is $V_0 = 610$ mV, and the threshold value is $V_{hc} = 320$ mV. The perturbation amplitude is $A = -200$ mV, and the pulse duration is 1 s. The corresponding chloride ions' concentrations are 0.015, 0.035, and 0.055 M, respectively. (d) The experimentally generated CCC as a function of noise level (chloride ions' concentration) for the subthreshold aperiodic signal perturbation. The indicated points (a)–(c) correspond to the anodic current time series shown in the left panels. This curve has a unimodal shape confirming the emergence of an intrinsic aperiodic stochastic resonance in the noise provoked dynamics.

(a) that there is no invoked system response for a low noise level, whereas there is an excellent correspondence between the system response and the subthreshold signal at an optimal noise level in panel (b). In panel (c), the subthreshold signal is completely shrouded by the stochastic system response.

In this case, to measure the information transfer, we use the CCC defined by

$$\mathrm{CCC} = \frac{\mathrm{cov}(x,y)}{\sigma_x \sigma_y}, \tag{2}$$

where x represents the time series of the aperiodic input signal, y represents the time series of the system response, σ_x and σ_y are their corresponding standard deviations, and $\mathrm{cov}(x,y)$ is the covariance between the input and the output. This coefficient quantifies the level of correlation between the subthreshold aperiodic input signal and the internal noise-induced system response. Figure 3(d) shows the CCC as a function of the chloride ions' concentration. The curve exhibits a unimodal profile where the maximum corresponds to the optimal noise level for which the maximum information transfer is observed. Points (a)–(c) correspond to the time series shown in the left panels.

In the second part of this set of experiments, we used the output of a deterministic model that simulates irregular neural spiking [27] as the subthreshold aperiodic signal. We use the times between these excitation pulses and generated a rectangular train of pulses with the same distribution. The spikes of the chaotic time series have an amplitude of $A = -200$ mV. Although the origin of the irregular spiking is purely deterministic, the histogram for the interspike intervals seems to fit well with a Poisson distribution [27]. As before, an identical subthreshold aperiodic deterministic spike train was superimposed upon the setpoint voltage V_0. Subsequently, we increased the level of noise by using higher chloride ions' concentrations in a sequence of experiments and measured the system response.

Figures 4(a)–4(c) show the stimulus-response time series for (a) low, (b) medium, and (c) high levels of internal noise. As before, it is observed that there is an optimal noise level, panel (b), that gives rise to an excellent stimulus-response correspondence, whereas a lower level (a) induces no response in the electrochemical system. On the contrary, when the noise level is high (c), there is no trace of input signal profile in the invoked dynamics. Figure 4(d) shows the CCC as a function of the chloride ions' concentration, quantifying the input-output correlation for experimental runs with the same setpoint voltage V_0. As in the earlier experiments with a subthreshold stochastic signal, the curve exhibits a maximum where the information transfer has reached an optimal value. Curves shown in Figs. 3(d) and 4(d) indicate the emergence of an intrinsic aperiodic stochastic resonance (IASR).

Our experimental results show evidence of the existence of intrinsic stochastic resonance in an electrochemical cell. This was confirmed quantitatively by calculating the signal to noise ratio (IPSR) and the cross-correlation coefficient (IASR) versus the amplitude of the internal noise (chloride ions' concentration) curves. Furthermore, the different combinations of the experimental configuration were tested

to validate the generic nature of the observed phenomenon. The images obtained from the electrode surface (SEM) when the periodic scenario is analyzed, reveal qualitatively the presence of an optimal level of noise wherein the surface roughness has reached a minimum deviation, i.e., is smooth. In the case of the subthreshold aperiodic signals, this image analysis is not considered appropriate to validate the quantitative analysis (CCC). Our results add credence to the belief that intrinsic noise, if judiciously employed, can indeed play a constructive role in nonlinear systems. In particular, an enhancement of information transfer efficiency is observed for an optimal value of internal noise. It is possible to envisage that numerous natural and biological systems use this feature in their daily functionalities. This, perhaps, entails regulating their levels of internal noise to optimize the system performance. Our future experiments would involve devising a technique wherein this resonance phenomenon can be invoked without varying the amplitude of the internal noise. This would be of relevance to natural systems where internal noise cannot be regulated.

We would like to thank CONACyT (México) and DST (India) for financial assistance.

[1] R. Benzi, A. Sutera, and A. Vulpiani, J. Phys. A **14**, L453 (1981).
[2] R. Benzi, G. Parisi, A. Sutera, and A. Vulpiani, Tellus **34**, 10 (1982).
[3] C. Nicolis and G. Nicolis, Tellus **33**, 225 (1981).
[4] A. Föster, M. Merget, and F. W. Schneider, J. Phys. Chem. **100**, 4442 (1996).
[5] T. Amemiya, T. Ohmori, M. Nakaiawa, and T. Yamaguchi, J. Phys. Chem. **102**, 4537 (1998).
[6] A. Longtin, A. Bulsara, and F. Moss, Phys. Rev. Lett. **67**, 656 (1991).
[7] B. Lindner, A. Longtin, and A. Bulsara, Neural Comput. **15**, 1761 (2003).
[8] B. Lindner, L. Schimansky-Geier, and A. Longtin, Phys. Rev. E **66**, 031916 (2002).
[9] J. J. Collins, C. C. Chow, A. C. Capela, and T. T. Imhoff, Phys. Rev. E **54**, 5575 (1996).
[10] L. Gammaitoni, P. Hanggi, P. Jung, and F. Marchesoni, Rev. Mod. Phys. **70**, 223 (1998).
[11] G. Giacomelli, M. Giudici, S. Balle, and J. R. Tredicce, Phys. Rev. Lett. **84**, 3298 (2000).
[12] H. Gang, T. Ditzinger, C. Z. Ning, and H. Haken, Phys. Rev. Lett. **71**, 807 (1993).
[13] A. S. Pikovsky and J. Kurths, Phys. Rev. Lett. **78**, 775 (1997).
[14] I. Z. Kiss, J. L. Hudson, G. J. Escalera Santos, and P. Parmananda, Phys. Rev. E **67**, 035201(R) (2003).
[15] P. Jung and J. W. Shuai, Europhys. Lett. **56**, 29 (2001).
[16] G. Schmid, I. Goychuk, and P. Hanggi, Europhys. Lett. **56**, 22 (2001).
[17] W. C. Stacey and D. M. Durand, J. Neurophysiol. **86**, 1104 (2001).
[18] G. Winterer, M. Ziller, H. Dorn, K. Frick, C. Mulert, N. Dahhan, W. M. Herrmann, and R. Coppola, Clin. Neurophysiol. **110**, 1193 (1999).
[19] H. Li, J. Ma, Z. Hou, and H. Xin, Acta Physico-Chimica Sinica **24**, 2203 (2008).
[20] M. D. McDonnell and L. M. Ward, Nat. Rev. Neurosci. **12**, 415 (2011).
[21] M. Rivera, G. J. Escalera Santos, J. Uruchurtu-Chavarín, and P. Parmananda, Phys. Rev. E **72**, 030102(R) (2005).
[22] D. Sazou, K. Michael, and M. Pagitsas, Electrochim. Acta **119**, 175 (2014).
[23] U. Bertocci, Corrosion **35**, 211 (1979).
[24] S. B. Lalvani and G. Zhang, Corr. Sci. **37**, 1583 (1995).
[25] G. J. Escalera Santos, M. Rivera, M. Eiswirth, and P. Parmananda, Phys. Rev. E **70**, 021103 (2004).
[26] B. McNamara, K. Wiesenfeld, and R. Roy, Phys. Rev. Lett. **60**, 2626 (1988).
[27] G. Baier, G. J. Escalera Santos, H. Perales, M. Rivera, M. Müller, R. Leder, and P. Parmananda, Phys. Rev. E **62**, R7579(R) (2000).